7 Simulated moving bed and related techniques

LUÍS S. PAIS, VERA G. MATA and ALÍRIO E. RODRIGUES

7.1 Overview

In the last 12 years, Simulated Moving Bed (SMB) technology has received considerable attention in both academic and industrial fields. The objective of this chapter is to introduce the SMB concept and to present the modeling strategies to simulate and to implement the design of SMB processes. Results will be shown, illustrating the influence of equilibrium adsorption isotherms and mass transfer resistances on SMB performance. At the end of the chapter, two examples of SMB-related techniques will be discussed: the Varicol process, to be used in SMB units with a low number of chromatographic columns; and the pseudo-SMB process, a modification of classic SMB operation to perform ternary separations.

7.2 The SMB concept

Adsorption and chromatographic processes are widely used in chemical industry for separation, purification and recovery. Extensive reviews concerning adsorption techniques with applications in the field of preparative and production scale chromatography can be found in literature [1–7]. Adsorption processes are generally more complex than the more conventional separation techniques such as fractional distillation, solvent-aided separations, or crystallization. However, separation by adsorption can be achieved for some systems, which are either difficult or impossible to obtain by other simple methods [8,9].

SMB is one of the most powerful techniques for preparative scale chromatography. The concept of SMB chromatography has been known since 1961 when the first patent by UOP (Universal Oil Products, Illinois, USA) appeared [10]. This technology was originally developed in the areas of petroleum refining and petrochemicals, and became generally known as the Sorbex process. Recently, SMB technology has found new successful applications in the areas of biotechnology, pharmaceuticals and fine chemistry. Following the increasing interest in preparative chromatographic separations, other companies developed alternative SMB schemes and applications. For example, several pharmaceutical companies and custom chemical manufactures are installing commercial-scale SMB units for producing pure enantiomeric compounds. Large-scale chromatographic separations were in the past limited mainly because of the high cost of the adsorbent, the high dilution of products and the large amount of mobile phase needed. With the introduction of the SMB technology, large-scale separations can now be carried out under cost-effective conditions. Concerning the pharmaceutical industry and the production of enantiomeric pure products, preparative enantioselective chromatography by SMB technology is now considered as an alternative to the enantioselective synthesis or diastereoisomeric crystallization.

The concept of SMB operation is based on the countercurrent contact between the liquid and the solid phases so that the mass transfer driving force can be maximized, leading to a significant reduction in mobile and stationary phase consumption when compared to classic elution chromatography. The principle of SMB operation can, in this way, be best understood by reference to the equivalent true moving bed (TMB) process. In the ideal TMB operation (see Fig. 7.1), liquid and solid flow in opposite directions, and are continuously recycled: the liquid flowing out of section 4 is recycled to section 1, while the solid coming out of section 1 is recycled to section 4. The feed is continuously injected in the middle of the system, between sections 2 and 3, and two product lines can be continuously collected: the extract, rich in the compounds that are more retained and so preferentially carried out with the solid phase; and the raffinate, rich in the less retained species that move upwards with the liquid phase. Pure eluent is continuously injected at the beginning of section 1, with the liquid recycled from the end of section 4.

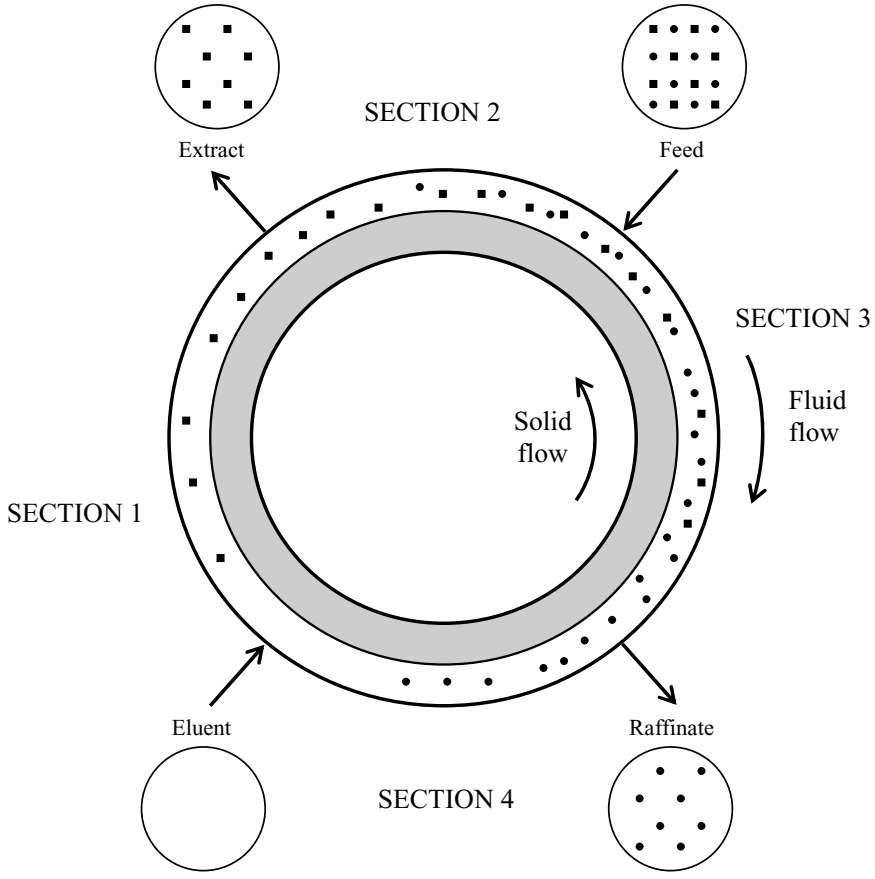

Figure 7.1 Schematic diagram for TMB operation.

Because of the addition and withdrawal of the four streams (eluent, extract, feed and raffinate), the TMB unit is divided into four sections: section 1, begins with the eluent inlet and ends in the extract withdrawal point; section 2, begins after the extract withdrawal point and ends just before the feed inlet; section 3, begins with the feed inlet and ends at the raffinate withdrawal point; and section 4, begins after the withdrawl point and ends just before the eluent inlet.

In the TMB operation, the solid flow-rate is constant all over the unit. However, because of the injection and withdrawal points, the liquid flow rates differ from section to section. This fact enables the four sections of the unit to perform different functions. To simplify the description of the function of each section, let us consider a feed mixture containing only two components: component A, the less adsorbed species and preferentially recovered in the raffinate, and component B, the more retained species and desirably recovered in the extract (see Fig. 7.2). In sections 2 and 3, the two components must move in opposite directions. The less retained component A must be desorbed and carried with the liquid phase, while the more retained species B must be adsorbed and carried with the solid phase. Considering that in these zones the objective is to prevent the contamination of the extract and raffinate streams by the undesired component, we can summarize saying that section 2 is the zone of desorption of the less retained species A, while section 3 is the zone of adsorption of the more retained component B. In section 4 both components must be adsorbed in order to regenerate the eluent that will be recycled to the first zone. Since the component A is the less retained species, the conditions for adsorption of this component will also allow the adsorption of the more retained species. On the other hand, section 1 is the zone of solid regeneration. In this section, both components must be desorbed in order to obtain a solid phase free from both components at the beginning of this zone. Since component B is the more retained species, the conditions for desorption of this component will also allow the desorption of the less retained component.

Unfortunately, the operation of this ideal TMB unit introduces problems concerning the movement of the solid phase. A uniform flow of both solid and liquid is difficult to obtain and also mechanical erosion of the adsorbent phase will occur. In view of these difficulties, an SMB technique was developed in order to retain the process advantages of continuous and countercurrent flow without introducing the problems associated with the actual movement of the solid phase (Fig. 7.3). In the SMB system the solid phase is fixed and the

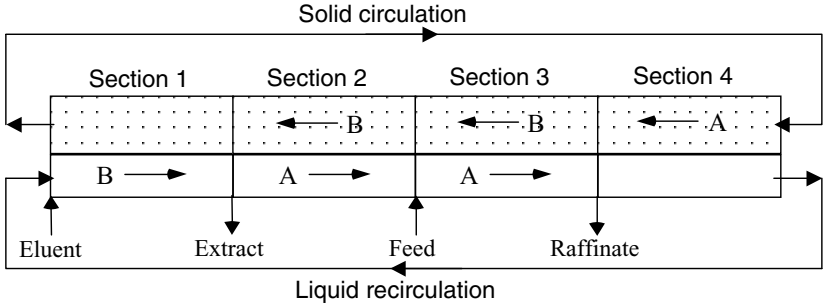

Figure 7.2 Desired net fluxes of a two species feed in each section of a TMB unit.

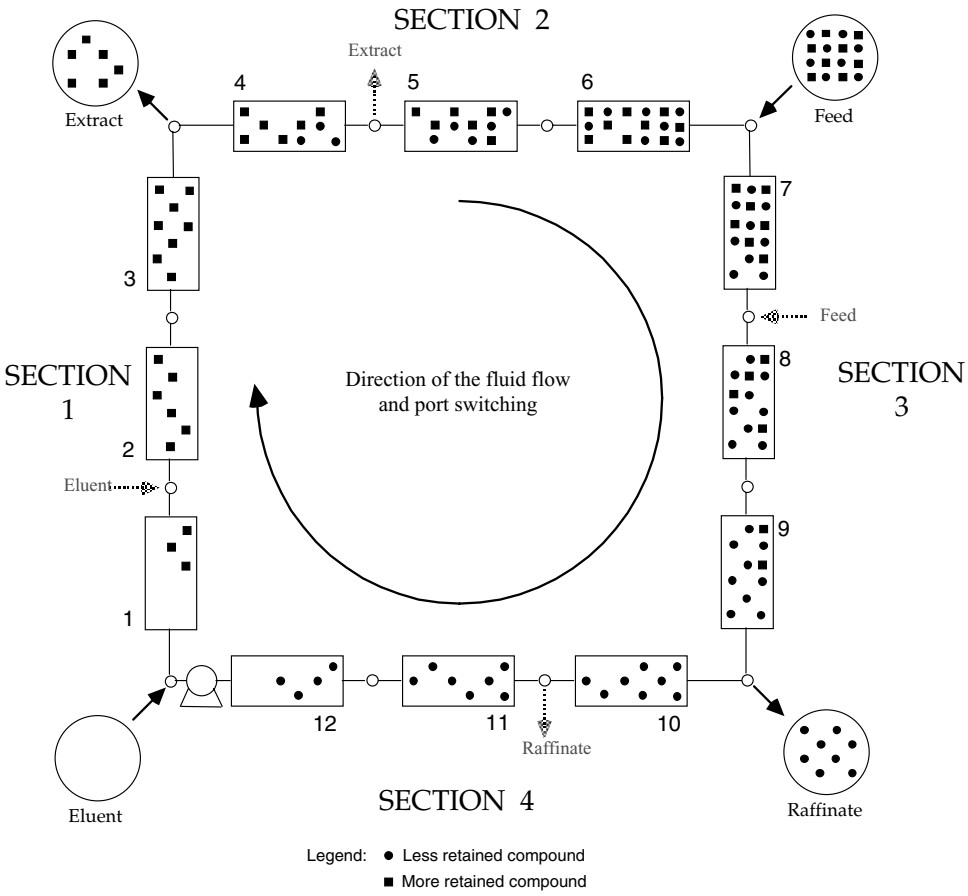

Figure 7.3 Schematic diagram for SMB operation.

positions of the inlet and outlet streams move periodically. This shift, carried out in the same direction of the liquid phase, simulates the movement of the solid phase in the opposite direction. Obviously, it is impractical to move the liquid inlet and withdrawal positions continuously. Nevertheless, approximately the same effect can be obtained by dividing the adsorbent bed into a number of fixed-bed columns and providing multiple access lines for the liquid streams between each column. Thereby, the four liquid access lines between each column can be used to perform a discreet movement of the inlet and outlet streams in the same direction of the liquid phase. In the Sorbex SMB technology developed by UOP, a complex rotary valve is used to periodically change the position of the eluent, extract, feed and raffinate lines along the adsorbent bed [10]. At any particular moment, only four lines between the rotary valve and the adsorbent bed are active. However, there are alternative techniques to perform the port switching, like the one developed by NovaSep (Vandoeuvre Les Nancy, France), a leading supplier of SMB industrial units that uses a set of individual on–off valves connecting the inlet and outlet streams to each node between columns.

7.3 Modeling of SMB processes

Following the two units described in the last section, the problem of modeling an SMB separation process can also be analyzed by two different strategies: one, by simulating the system directly, taking into account its intermittent behavior; other by representing its operation in terms of a true countercurrent system. The first model represents the real SMB and considers the periodic switch of the injection and collection points. The second is developed by assuming the equivalence with the TMB, where solid and fluid phases flow in opposite directions. Both mathematical models are based on the following assumptions: an axially dispersed plug flow model is used to describe the fluid phase flow; a plug flow model is used to represent the countercurrent solid flow in the TMB approach; the adsorbent particles are considered as homogeneous material and mass transfer between fluid and solid is described by the linear driving force model. The adsorption equilibrium isotherms can be described by any kind of model, such as, linear, Langmuir, linear plus Langmuir, or bi-Langmuir models.

The transient SMB and TMB model equations are summarized in Table 7.1, which includes a mass balance over a volume element of the bed, a mass balance in the particle, initial and boundary conditions, global balances at each node, and the adsorption equilibrium isotherms. It should be pointed out that, owing to the switch of inlet and outlet lines, each fixed-bed column of an SMB unit travels through different sections, playing different functions during a whole cycle. In this way, the boundary conditions for each column change after the end of each switch time interval. This time dependence of the boundary conditions leads to a cyclic steady state for the SMB operation, instead of a real steady state achieved for the TMB model. In the TMB model, the solid phase is assumed to move in plug flow in the opposite direction to the fluid phase, while the inlet and outlet lines remain fixed. Model equations for the TMB model are equivalent to those presented for the SMB model, but include the term that represents the countercurrent movement of the solid phase. The resulting model parameters are the following: the ratio between solid and fluid volumes, $(1-\varepsilon)/\varepsilon$; the ratio between fluid and solid interstitial velocities, $\gamma_j = v_j/u_s$; the Peclet number, $Pe_j = v_j L_j/D_{Lj}$; the number of mass transfer units, $n_i = kL_j/u_s$; and the adsorption equilibrium parameters.

Table 7.1 Transient SMB and TMB model equations

Simulated moving bed model equations

Mass balance over a volume element of the bed k:

$$\frac{\partial C_{ik}}{\partial \theta} = \gamma_k^* \left\{ \frac{1}{Pe_k} \frac{\partial^2 C_{ik}}{\partial x^2} - \frac{\partial C_{ik}}{\partial x} \right\} - \frac{(1-\varepsilon)}{\varepsilon} n_k (q_{ik}^* - q_{ik}) \tag{7.1a}$$

Mass balance in the particle:

$$\frac{\partial q_{ik}}{\partial \theta} = n_k (q_{ik}^* - q_{ik}) \tag{7.1b}$$

Initial conditions:

$$\theta = 0: \qquad C_{ik} = q_{ik} = 0 \tag{7.2}$$

Boundary conditions for column k:

$$x = 0: \qquad C_{ik} - \frac{1}{Pe_k} \frac{\mathrm{d}C_{ik}}{\mathrm{d}x} = C_{ik,0} \tag{7.3}$$

Continued

Table 7.1 *Continued*

where $C_{ik,0}$ is the inlet concentration of species i in column k.
$x = 1$:
For a column inside a section and for extract and raffinate nodes: $C_{ik} = C_{ik+1,0}$ (7.4a)
For the eluent node: $C_{ik} = \dfrac{\nu_1^*}{\nu_4^*} C_{ik+1,0}$ (7.4b)
For the feed node: $C_{ik} = \dfrac{\nu_3^*}{\nu_2^*} C_{ik+1,0} - \dfrac{\nu_\mathrm{F}}{\nu_2^*} C_i^\mathrm{F}$ (7.4c)

Global balances:
Eluent node: $\nu_1^* = \nu_4^* + \nu_\mathrm{E}$ (7.5a)
Extract node: $\nu_2^* = \nu_1^* - \nu_\mathrm{X}$ (7.5b)
Feed node: $\nu_3^* = \nu_2^* + \nu_\mathrm{F}$ (7.5c)
Raffinate node: $\nu_4^* = \nu_3^* - \nu_\mathrm{R}$ (7.5d)

Multicomponent adsorption equilibrium isotherm:
$q_{\mathrm{A}k}^* = f_\mathrm{A}(C_{\mathrm{A}k}, C_{\mathrm{B}k})$ (7.6a)
$q_{\mathrm{B}k}^* = f_\mathrm{B}(C_{\mathrm{A}k}, C_{\mathrm{B}k})$ (7.6b)

True moving bed model equations

Mass balance over a volume element of the bed j:
$$\frac{\partial C_{ij}}{\partial \theta} = \gamma_j \left\{ \frac{1}{Pe_j} \frac{\partial^2 C_{ij}}{\partial x^2} - \frac{\partial C_{ij}}{\partial x} \right\} - \frac{(1-\varepsilon)}{\varepsilon} n_j (q_{ij}^* - q_{ij}) \quad (7.7a)$$

Mass balance in the particle:
$$\frac{\partial q_{ij}}{\partial \theta} = \frac{\partial q_{ij}}{\partial x} + n_j (q_{ij}^* - q_{ij}) \quad (7.7b)$$

Initial conditions:
$\theta = 0$: $C_{ij} = q_{ij} = 0$ (7.8)

Boundary conditions for column k:
$$x = 0: \quad C_{ij} - \frac{1}{Pe_j} \frac{\mathrm{d}C_{ij}}{\mathrm{d}x} = C_{ij,0} \quad (7.9)$$
where $C_{ij,0}$ is the inlet concentration of species i in section j.
$x = 1$:
For the eluent node: $C_{i4} = \dfrac{\nu_1}{\nu_4} C_{i1,0}$ (7.10a)
For the extract node: $C_{i1} = C_{i2,0}$ (7.10b)
For the feed node: $C_{i2} = \dfrac{\nu_3}{\nu_2} C_{i3,0} - \dfrac{\nu_\mathrm{F}}{\nu_2} C_i^\mathrm{F}$ (7.10c)
For the raffinate node: $C_{i3} = C_{i4,0}$ (7.10d)
and $q_{i4} = q_{i1,0}$, $q_{i1} = q_{i2,0}$, $q_{i2} = q_{i3,0}$, $q_{i3} = q_{i4,0}$ (7.10e)

Global balances:
Eluent node: $\nu_1 = \nu_4 + \nu_\mathrm{E}$ (7.11a)
Extract node: $\nu_2 = \nu_1 - \nu_\mathrm{X}$ (7.11b)
Feed node: $\nu_3 = \nu_2 + \nu_\mathrm{F}$ (7.11c)
Raffinate node: $\nu_4 = \nu_3 - \nu_\mathrm{R}$ (7.11d)

Multicomponent adsorption equilibrium isotherm:
$q_{\mathrm{A}j}^* = f_\mathrm{A}(C_{\mathrm{A}j}, C_{\mathrm{B}j})$ (7.12a)
$q_{\mathrm{B}j}^* = f_\mathrm{B}(C_{\mathrm{A}j}, C_{\mathrm{B}j})$ (7.12b)

The equivalence between the TMB and the SMB models is made by keeping constant the liquid velocity relative to the solid velocity; that is, the liquid velocity in the SMB system is equal to the sum of liquid and solid velocities in the TMB model, $v_j^* = v_j + u_\mathrm{s}$. Also, the solid velocity in the TMB model must be evaluated from the value of the switch time interval t^* of the SMB model, as $u_\mathrm{s} = L_\mathrm{c}/t^*$, where L_c is the length of one SMB column.

This implies that the internal liquid flow rates in both systems are not the same, but related by $Q_j^* = Q_j + \varepsilon V_c/t^*$, where Q_j^* and Q_j are the internal liquid flow rates in the SMB and TMB models, respectively, and V_c is the volume of one SMB column.

The differences between SMB and TMB model predictions, in terms of steady-state internal concentration profiles and also in terms of process performance like purity and recovery, depend on the number of subdivisions used in the SMB unit. In fact, the similarity would be perfect if the adsorbent bed of the SMB unit were divided into an infinite number of fixed-bed columns and using an infinitesimal switch time interval. Fortunately, a small subdivision of the bed is sufficient to ensure that an SMB unit performs close to the ideal TMB countercurrent operation. We concluded that the prediction of the SMB operation can be carried out through the equivalent TMB approach when the SMB unit is constituted by, at least, two columns per section (a total of eight columns) [11]. However, we should not forget that recent applications in the pharmaceutical industry use SMB systems containing a low total number of columns, for instance, a total of five or six columns. In these cases, as it was shown recently [12], the real and more precise SMB model should be used. Also, the SMB model will always be useful in characterizing the dynamic cyclic behavior of the concentration profiles. On the other hand, if the subdivision of the bed is sufficient, we shall use the simple TMB model, with obvious advantages in computing timesavings. Moreover, if we are interested to characterize only the steady-state operation, we can develop a steady-state TMB model that is simpler to implement. In fact, the original problem represented by a set of partial differential equations will be simplified to a set of ordinary differential equations. Other simplifications that can be introduced consist in neglecting axial dispersion and mass transfer resistances, leading to an equilibrium model [13,14] that, under certain kind of adsorption equilibrium isotherms, can lead to explicit criteria for the choice of the SMB operating conditions for complete separation of a binary mixture.

7.4 Design of SMB processes

The design problem of an SMB unit consists in setting the flow-rates in each section and the value for the switch time interval to obtain the desired separation. Following the equivalence to the TMB operation, some constraints have to be met if one wants to recover the less adsorbed component A in the raffinate and the more retained component B in the extract. As it was pointed out earlier (see Fig. 7.2), these constraints can be expressed in terms of the net fluxes of each component in each section:

$$\frac{Q_1 c_{B1}}{Q_S q_{B1}} > 1 \qquad \frac{Q_2 c_{A2}}{Q_S q_{A2}} > 1 \quad \text{and} \quad \frac{Q_2 c_{B2}}{Q_S q_{B2}} < 1 \tag{7.13}$$

$$\frac{Q_3 c_{A3}}{Q_S q_{A3}} > 1 \quad \text{and} \quad \frac{Q_3 c_{B3}}{Q_S q_{B3}} < 1 \qquad \frac{Q_4 c_{A4}}{Q_S q_{A4}} < 1$$

where Q_1, Q_2, Q_3, Q_4 are the volumetric liquid flow-rates in the various sections of the TMB, Q_S is the solid flow rate, c_{Aj}, c_{Bj} are the concentrations of species A and B in the liquid phase and q_{Aj}, q_{Bj} are the adsorbed concentrations of components A and B, in section j. The same constraints can be expressed alternatively in terms of fluid and solid interstitial velocities. Using the dimensionless model parameters defined earlier – $\gamma_j = v_j/u_s$, as the

ratio between fluid and solid interstitial velocities in zone j; and $\varepsilon/(1-\varepsilon)$, as the ratio between fluid and solid volumes, the constraints defined by Equation (7.13) become

$$\gamma_1 > \frac{1-\varepsilon}{\varepsilon}\frac{q_{B1}}{c_{B1}} \qquad \frac{1-\varepsilon}{\varepsilon}\frac{q_{A2}}{c_{A2}} < \gamma_2 < \frac{1-\varepsilon}{\varepsilon}\frac{q_{B2}}{c_{B2}} \tag{7.14}$$

$$\frac{1-\varepsilon}{\varepsilon}\frac{q_{A3}}{c_{A3}} < \gamma_3 < \frac{1-\varepsilon}{\varepsilon}\frac{q_{B3}}{c_{B3}} \qquad \gamma_4 < \frac{1-\varepsilon}{\varepsilon}\frac{q_{A4}}{c_{A4}}$$

For the case of a binary system with linear adsorption isotherms, $q_{ij}/c_{ij} = K_i$ is constant, and very simple formulas can be derived to evaluate the TMB flow rates [15]. For nonlinear systems, however, the evaluation of the flow rates is not straightforward. It is well known that the adsorption behavior must be commonly described with more complex models, such as the nonlinear competitive adsorption isotherm. For this kind of system, the adsorbed concentration of a component in equilibrium with its concentration in the liquid phase depends not only on its own but also on the concentration of all other species. This means that the ratio between the adsorbed-phase and fluid-phase concentrations that influences the net fluxes of both components in the TMB operation [see Equations (7.13) or (7.14)] is no longer constant but concentration-dependent.

Morbidelli and coworkers developed a complete design of the binary countercurrent separation processes by SMB chromatography in the frame of equilibrium theory, assuming that mass transfer resistances and axial dispersion are negligible, and that the adsorption equilibria can be described through a variable selectivity modified Langmuir isotherm [14]. The conditions to achieve complete separation were evaluated considering the equivalent TMB operation and defining a region for complete separation in terms of the flow-rate ratios in the four sections of this equivalent TMB unit. This separation region is the area in a $\gamma_3 \times \gamma_2$ plot where both extract and raffinate are pure (γ_2 and γ_3 are the ratios between fluid and solid interstitial velocities in sections 2 and 3, respectively). This plot, first proposed by Morbidelli and coworkers [13,14], is an important tool in the choice of the best operating conditions, providing that the constraints in sections 1 and 4 are fulfilled; that is, the flow rate ratios in sections 1 and 4, γ_1 and γ_4, are chosen away from their critical values. Figure 7.4 shows a typical $\gamma_3 \times \gamma_2$ plot that can be found for a nonlinear TMB separation. Depending on the γ_2 and γ_3 values, we can find four regions: one where none of the extract and raffinate streams are pure, two regions where only one of the two streams is pure, and one region where both of the extract and raffinate streams are pure. Of course, we must operate the system with operating conditions inside this last region, called the separation region, since the natural objective is to obtain simultaneously pure extract and raffinate streams. Moreover, we should operate the system with operating conditions near the vertex point of this separation region. The vertex is the point at the boundary of the separation region most distant from the diagonal $\gamma_3 = \gamma_2$ (see Fig. 7.4), and represents the best operating conditions in terms of system productivity and solvent consumption. In fact, system productivity can be defined as the total amount of feed introduced in the system per volume of adsorbent bed and per unit of time, and is proportional to the difference $\gamma_3 - \gamma_2$.

The separation regions, originally built by using the equilibrium theory model, can also be evaluated using more precise models that take into account the resistances to mass transfer [16–20]. The presence of mass transfer resistance can affect significantly the performance of the SMB operation, reducing the size of the separation region and modifying the optimum SMB operating conditions [16,17,21]. Moreover, when mass transfer resistance

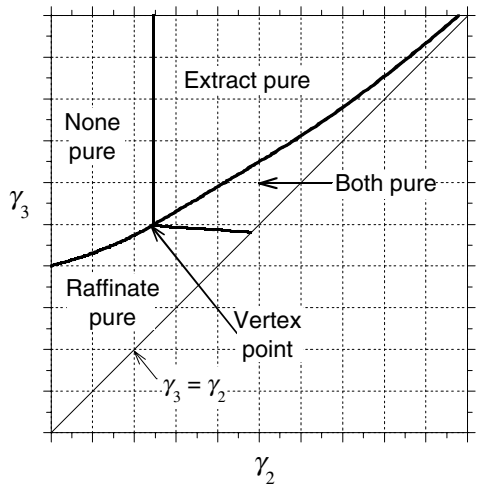

Figure 7.4 Typical $\gamma_3 \times \gamma_2$ plot for nonlinear TMB operation.

is neglected, equilibrium theory states that the critical flow rate ratios required to achieve separation depend exclusively on the equilibrium data. However, in the presence of mass transfer resistance, those critical values are more restrictive and should be evaluated through simulation [22–24].

7.5 Simulation of SMB processes

The TMB and SMB models presented can be used to study the influence of the various model parameters on the system performance. System performance can be evaluated by using the following three main parameters: purity, productivity and solvent consumption.

(a) Purity:

$$\text{Extract purity} = \frac{C_{\mathrm{B}}^{\mathrm{X}}}{C_{\mathrm{A}}^{\mathrm{X}} + C_{\mathrm{B}}^{\mathrm{X}}} \tag{7.15}$$

$$\text{Raffinate purity} = \frac{C_{\mathrm{A}}^{\mathrm{R}}}{C_{\mathrm{A}}^{\mathrm{R}} + C_{\mathrm{B}}^{\mathrm{R}}} \tag{7.16}$$

(b) Productivity:

$$\mathrm{pr} = \frac{Q_{\mathrm{F}}(C_{\mathrm{A}}^{\mathrm{F}} + C_{\mathrm{B}}^{\mathrm{F}})}{V_{\mathrm{T}}} = \frac{\varepsilon}{N_{\mathrm{c}} t^*}(\gamma_3 - \gamma_2)\left(C_{\mathrm{A}}^{\mathrm{F}} + C_{\mathrm{B}}^{\mathrm{F}}\right) \tag{7.17}$$

$$\pi = \mathrm{pr}\frac{N_{\mathrm{c}} t^*}{\varepsilon} = (\gamma_3 - \gamma_2)\left(C_{\mathrm{A}}^{\mathrm{F}} + C_{\mathrm{B}}^{\mathrm{F}}\right) \tag{7.18}$$

(c) Solvent consumption:

$$\mathrm{sc} = \frac{Q_{\mathrm{E}} + Q_{\mathrm{F}}}{Q_{\mathrm{F}}\left(C_{\mathrm{A}}^{\mathrm{F}} + C_{\mathrm{B}}^{\mathrm{F}}\right)} = \frac{1}{\left(C_{\mathrm{A}}^{\mathrm{F}} + C_{\mathrm{B}}^{\mathrm{F}}\right)}\left(1 + \frac{\gamma_1 - \gamma_4}{\gamma_3 - \gamma_2}\right) \tag{7.19}$$

This section will present the results obtained using the equivalent countercurrent TMB model to study the influence of two main model parameters: the adsorption isotherm parameters and the mass transfer coefficient (mass transfer resistance). A more complete study of the influence of other model parameters can be found elsewhere [16,25].

7.5.1 *Influence of the equilibrium adsorption isotherms*

A binary linear + Langmuir isotherm model is used as illustrative example:

$$q_i^* = mC_i + \frac{Qb_iC_i}{1 + b_AC_A + b_BC_B} \tag{7.20}$$

where $i = A, B$ represents the component (A is the less retained, B the more retained component). This model is often used to describe the adsorption isotherms for chiral mixtures, since it is a competitive model and can predict the concentration dependency of the selectivity factor:

$$\alpha = \frac{(q_B^*/C_B)}{(q_A^*/C_A)} = \frac{m(1 + b_AC_A + b_BC_B) + Qb_B}{m(1 + b_AC_A + b_BC_B) + Qb_A} \tag{7.21}$$

As shown by Equation (7.21), the selectivity factor depends on both species concentrations and is not constant like, for instance, for the competitive Langmuir isotherm model. At low concentrations, the adsorption isotherms are near linear and the previous equations become

$$q_{i,\text{linear}}^* = (m + Qb_i)C_i \tag{7.22}$$

$$K_i = \left.\frac{q_i^*}{C_i}\right|_{\text{linear}} = m + Qb_i \tag{7.23}$$

$$\alpha_{\text{linear}} = \frac{K_B}{K_A} = \frac{m + Qb_B}{m + Qb_A} \tag{7.24}$$

The examples shown in this section use isotherm parameters described in Table 7.2. Cases 1, 2 and 3 have the same m, Q and b_A parameters, but differ for b_B values. In consequence, K_A is the same for all cases, but not K_B, and so, α_{linear}. Figure 7.5 shows the system selectivity as a function of both species concentrations and illustrates three completely different situations.

Cases 1, 4 and 5 have the same m, but different Q, b_A and b_B parameters. However, the products Qb_A and Qb_B are the same for all situations and, consequently, they have the same K_A, K_B and α_{linear}. Figure 7.6 shows the system selectivity as a function of both component concentration for cases 1, 4 and 5. All cases show the same selectivity in the linear range of the adsorption isotherms (low concentrations), but present different values in the nonlinear region owing to different b_i values [see Equation 21]. This fact will influence the form of the separation regions, mainly for higher feed concentrations. The $\gamma_3 \times \gamma_2$ separation

Table 7.2 Linear + Langmuir isotherm parameters used in simulations

	Isotherm parameters				Linear range		
Case	m	Q (g/L)	b_A (L/g)	b_B (L/g)	K_A	K_B	α_{linear}
1	1.00	10.0	0.10	0.15	2.00	2.50	1.25
2	1.00	10.0	0.10	0.20	2.00	3.00	1.50
3	1.00	10.0	0.10	0.30	2.00	4.00	2.00
1	1.00	10.0	0.10	0.15	2.00	2.50	1.25
4	1.00	5.0	0.20	0.30	2.00	2.50	1.25
5	1.00	2.5	0.40	0.60	2.00	2.50	1.25

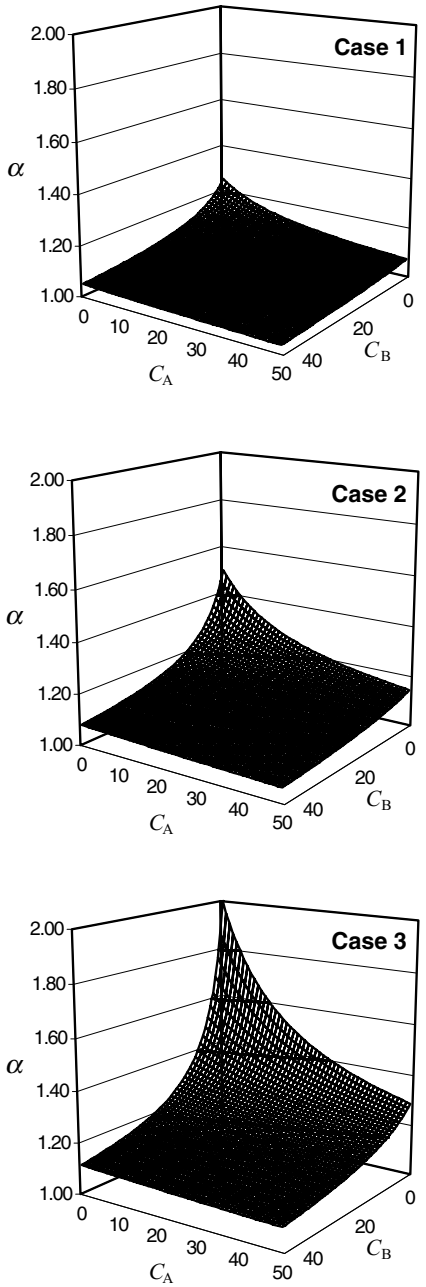

Figure 7.5 System selectivity α as a function of both species concentrations: cases 1, 2 and 3. For adsorption isotherm parameters, see Table 7.2.

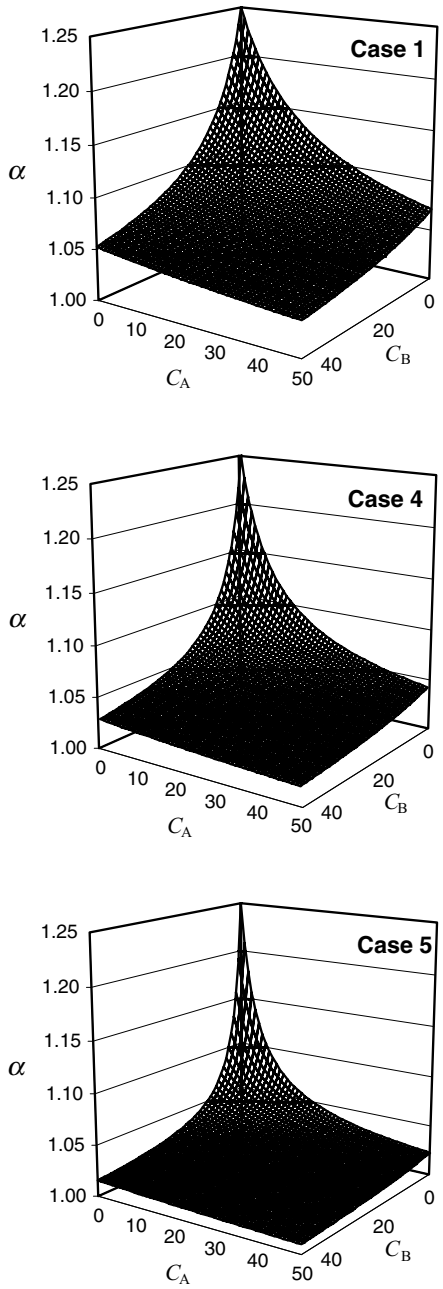

Figure 7.6 System selectivity α as a function of both species concentrations: cases 1, 4 and 5. For adsorption isotherm parameters, see Table 7.2.

regions were obtained using the equivalent countercurrent equilibrium theory model [14] (negligible axial dispersion and mass transfer resistances) with bed porosity $\varepsilon = 0.4$.

The influence of adsorption isotherm parameters on the $\gamma_3 \times \gamma_2$ separation region is shown in Fig. 7.7 for cases 1, 2 and 3, and for feed concentrations of $C_A^f = C_B^f = 0.1$, 2 and 10 g/L.

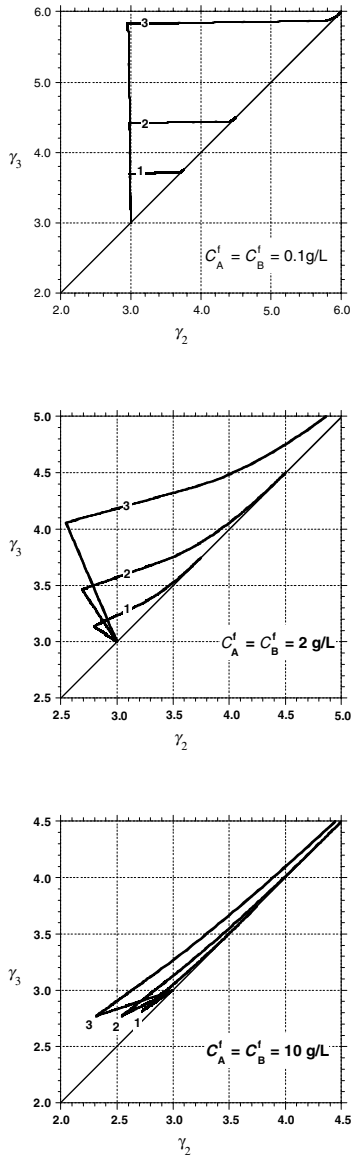

Figure 7.7 Influence of adsorption isotherms parameters on the $\gamma_3 \times \gamma_2$ separation region: cases 1, 2 and 3 for feed concentrations of $C_A^f = C_B^f = 0.1$, 2 and 10 g/L. Separation regions obtained using the equilibrium theory model. For adsorption isotherm parameters, see Table 7.2.

The typical rectangular triangles are obtained for the linear range of adsorption isotherms ($C_A^f = C_B^f = 0.1$ g/L); for higher concentrations, the area of separation regions diminishes and become more narrow and closer to the diagonal $\gamma_3 = \gamma_2$. Completely different situations are obtained for the three cases 1, 2 and 3, since adsorption isotherms are, also, significantly different. This difference also influences the system productivity and solvent consumption (see Fig. 7.8). Interesting results are obtained when we take into account the adsorption

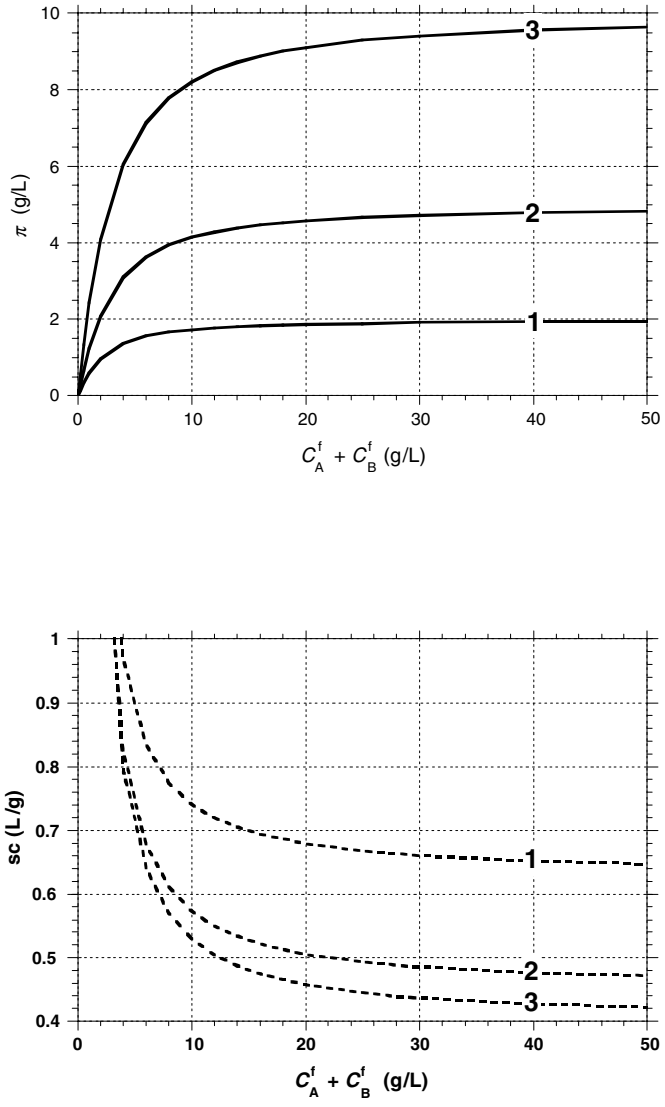

Figure 7.8 Influence of adsorption isotherms parameters on the system productivity and solvent consumption: cases 1, 2 and 3. System productivity and solvent consumption are evaluated at the vertex points of the separation regions obtained using the equilibrium theory model.

isotherm parameters for cases 1, 4 and 5. For low concentrations (see Fig. 7.9, $C_A^f = C_B^f = 0.1$ g/L), the $\gamma_3 \times \gamma_2$ separation region obtained for the three cases are not significantly different, when compared with the same situation for cases 1, 2 and 3 (compare Figs. 7.7 and 7.9, for $C_A^f = C_B^f = 0.1$ g/L). This occurs because cases 1, 4 and 5 have the same

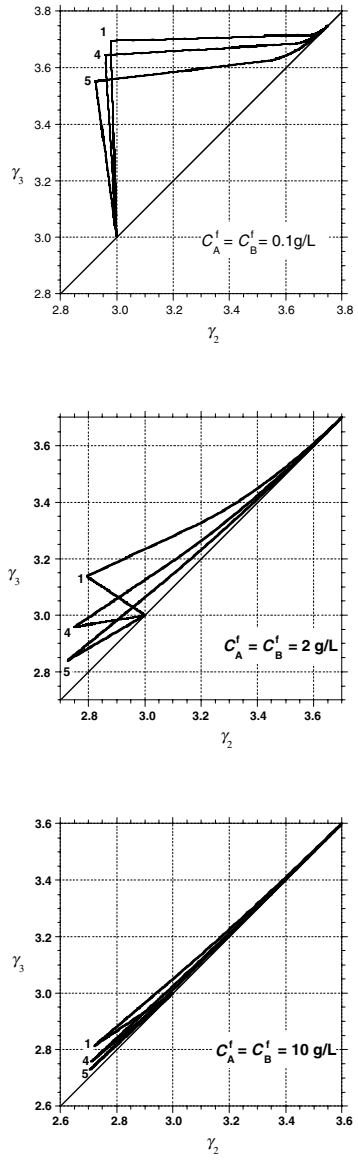

Figure 7.9 Influence of adsorption isotherms parameters on the $\gamma_3 \times \gamma_2$ separation region: cases 1, 4 and 5 for feed concentrations of $C_A^f = C_B^f = 0.1$, 2 and 10 g/L. Separation regions obtained using the equilibrium theory model. For adsorption isotherm parameters, see Table 7.2.

isotherm parameters in the linear range ($K_A = 2.00$, $K_B = 2.50$, $\alpha_{linear} = 1.25$). However, completely different separation regions are obtained for higher concentrations (see Figure 7.9, $C_A^f = C_B^f = 2$ and 10 g/L). Figure 7.10 shows that cases 1, 4 and 5 also present different behaviors in terms of system productivity and solvent consumption.

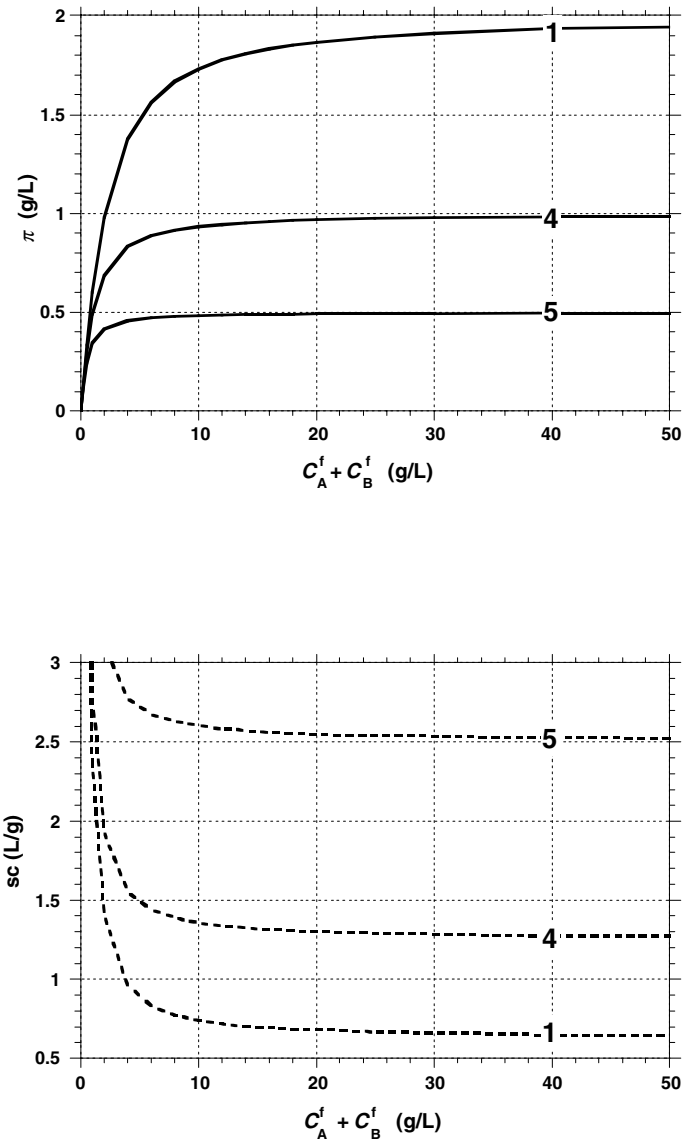

Figure 7.10 Influence of adsorption isotherms parameters on the system productivity and solvent consumption: cases 1, 4 and 5. System productivity and solvent consumption are evaluated at the vertex points of the separation regions obtained using the equilibrium theory model.

The previous results illustrate the crucial importance of the equilibrium adsorption isotherms on system performance. Also, it is shown that the evaluation of the SMB operation and system performance needs the complete knowledge of the equilibrium adsorption isotherms, not only in the linear range, but certainly in the nonlinear and competitive region.

7.5.2 *Influence of mass transfer resistance*

Case 1 (see Table 7.2) was used to study the influence of mass transfer resistance on the $\gamma_3 \times \gamma_2$ separation regions and on system productivity and solvent consumption. The separation regions were obtained by simulation using the TMB model presented in Section 7.2, which considers axial dispersion and mass transfer resistance. In all simulations, bed porosity was considered as $\varepsilon = 0.4$ and Peclet number as $Pe_j = 2000$ (negligible axial dispersion). The ratios between fluid and solid interstitial velocities in sections 1 and 4 were fixed away from their critical values ($\gamma_1 = 5.625$, $\gamma_4 = 2.000$).

Figure 7.11 shows the influence of mass transfer resistances (mass transfer coefficient, $k = 0.125, 0.15, 0.2$ and $0.4\ s^{-1}$) on the form of the $\gamma_3 \times \gamma_2$ separation regions for three feed concentrations: $C_A^f = C_B^f = 0.1$, 1 and 5 g/L. Inside each separation region both extract and raffinate are at least 99.0% pure. Also shown in each graph is the result obtained considering negligible mass transfer resistance ($k \to \infty$; equilibrium theory model). The conclusion is obvious: mass transfer resistance reduces the size of the separation region, diminishing the region of operating conditions that allow a certain purity criteria. This is true for both low and high concentrations, i.e. for both linear and nonlinear ranges of the equilibrium adsorption isotherms. Consequently, system productivity and solvent consumption are also influenced by mass transfer resistance (see Fig 7.12). The previous results show that when mass transfer resistance is important, we shall replace the use of the simple equilibrium theory model by a more realistic model that takes into account these phenomena.

7.6 SMB related techniques

SMB technology is one of the most powerful techniques for preparative chromatography. Recently, various authors and companies have proposed SMB-related techniques. Among them is the use of new operating strategies to be used in SMB units with a low number of chromatographic columns, and the modification of SMB operation to perform ternary separations.

7.6.1 *Varicol processes*

The Varicol process was recently proposed by NovaSep [26,27] and is based on a nonsynchronous shift of the inlet and outlet valves in a multicolumn system, in contrast to the SMB operation where this shift is synchronous. This new process makes possible operation with a number of columns per section that is not constant in time, and can show advantages over the classical SMB operation, particularly when using a low number of columns (recent applications in the pharmaceutical industry use SMB systems containing, usually, four to eight chromatographic columns).

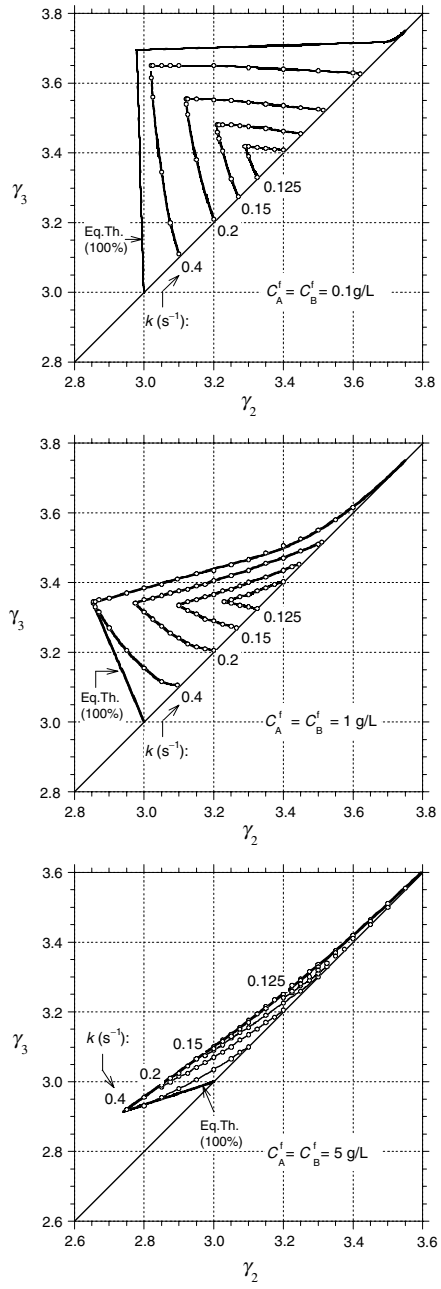

Figure 7.11 Influence of mass transfer resistance on the $\gamma_3 \times \gamma_2$ separation region for case 1 and feed concentrations of $C_A^f = C_B^f = 0.1$, 1 and 5 g/L. Separation regions obtained by simulation using the steady-state TMB model. Inside each separation region both extract and raffinate are, at least, 99.0% pure. Also shown is the separation region obtained using the equilibrium theory model ($k \to \infty$; 100% pure extract and raffinate).

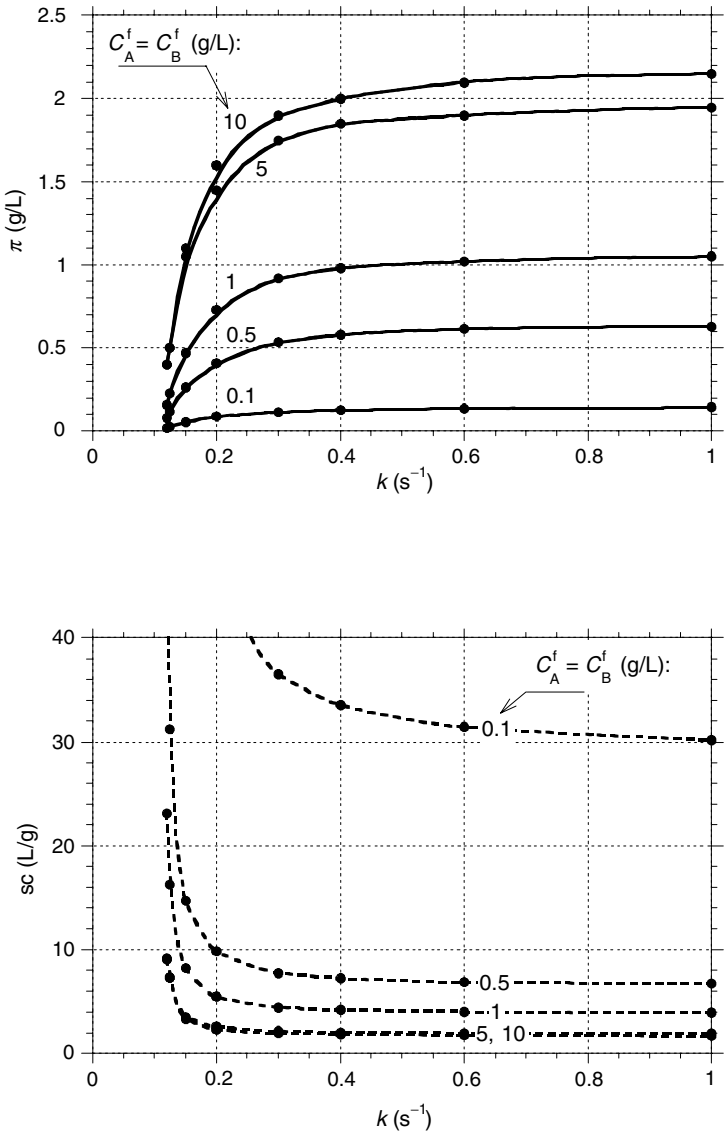

Figure 7.12 Influence of mass transfer resistance on the system productivity and solvent consumption for case 1 and feed concentrations of $C_A^f = C_B^f = 0.1$, 0.5, 1, 5 and 10 g/L. System productivity and solvent consumption are evaluated at the vertex points of the separation regions obtained by simulation using the steady-state TMB model.

Figure 7.13 shows an example of Varicol operation and compares it to the classic SMB system. Consider an SMB system with a 1211 configuration (see Fig. 7.13, left). At the beginning of each switch time interval ($\theta = 0$), all the inlet and outlet streams will jump one column forward, in the direction of the liquid phase. This jump is synchronous, and so, for this example, sections 1, 3 and 4 will always have one column, while section 2 will always have two. Consider now an SMB 1121 configuration: in this case, the feed inlet is at the

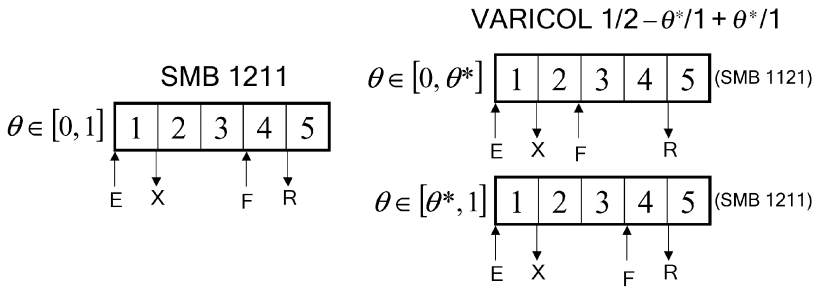

Figure 7.13 Example of a Varicol operation: five-column SMB 1211 configuration (left) and five-column Varicol $1/2 - \theta^*/1 + \theta^*/1$ configuration, with $0 \leq \theta^* \leq 1$ (right).

beginning of the third column (see Fig. 7.13, upper right). At a certain moment during the switch time interval ($0 \leq \theta = \theta^* \leq 1$), the feed inlet will jump to the beginning of the fourth column, while all the other lines (eluent, extract and raffinate) remain fixed (see Fig. 7.13, down right). From now on, the configuration is not 1121 but 1211, and will stay like this until the end of the switch time interval is reached. We may say that during the whole switch time interval we have two different SMB configurations: during the interval $0 \leq \theta < \theta^*$, the SMB 1121 configuration; during the interval $\theta^* \leq \theta \leq 1$, the SMB 1211 configuration. This example represents a Varicol operation, since the system is operating with a number of columns per section that is not constant in time. For this example, sections 1 and 4 always have one column; however, sections 2 and 3 have, respectively, $2 - \theta^*$ and $1 + \theta^*$ columns; that is, we are in the presence of a Varicol $1/2 - \theta^*/1 + \theta^*/1$ configuration.

As it was shown recently [12], the simulation of SMB units with a low number of chromatographic columns must use the real and more precise SMB model. Figure 7.14 illustrates this necessity: for a 1211 configuration (one column in sections 1, 3 and 4; two columns in section 2), a feed concentration of $C_A^f = C_B^f = 1$ g/L and a mass transfer coefficient of $k = 0.2\,s^{-1}$, there is no 99.0% separation region predicted by the real and more precise SMB model. However, completely different results are obtained if we wrongly use the TMB or the equilibrium theory approaches. Figure 7.14 clearly shows that the evaluation of the SMB units using a low number of chromatographic columns shall avoid the use of the ideal countercurrent TMB or equilibrium theory models, and a more realistic SMB model, which takes into account the periodic shift of the injection and collection points, is needed.

Figure 7.15 presents the 99.0% $\gamma_3 \times \gamma_2$ separation regions obtained for the same operating conditions of Fig. 7.14 but using the Varicol $1/2 - \theta^*/1 + \theta^*/1$ configuration. Model equations to simulate the Varicol process are the same as used in the SMB model, only they must take into account the nonsynchronous shift of the inlet and outlet lines. Figure 7.15 clearly shows the advantages of the Varicol operation when using a low number of columns, since complete different separation regions are obtained when changing the θ^* value (remember that no 99.0% separation region is obtained for any five-column classic SMB configuration). Figure 7.16 stresses the influence of Varicol configuration in terms of system productivity and solvent consumption. For this case, the best situation occurs for $\theta^* = 0.5$, i.e. for a Varicol 1/1.5/1.5/1 configuration. However, even better performance can be obtained by considering the optimization procedure as not confined to the two central sections, but as extended to the two adjacent sections, 1 and 4.

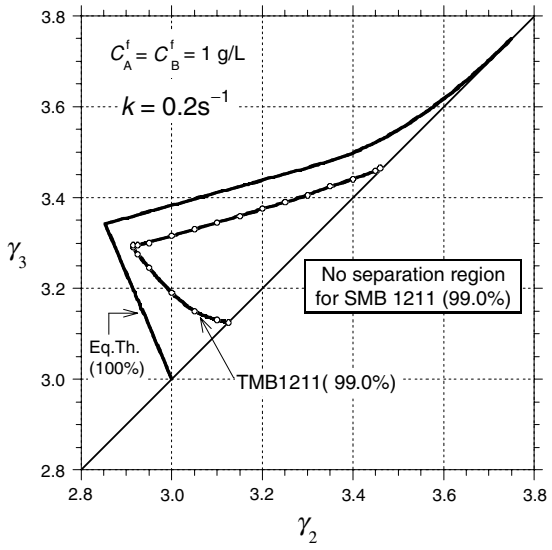

Figure 7.14 $\gamma_3 \times \gamma_2$ separation regions for case 1, feed concentrations of $C_A^f = C_B^f = 1$ g/L, and a 1211 configuration (a total of five columns, two columns in section 2). Shown are the separation regions obtained using the equilibrium model ($k \to \infty$; 100% pure extract and raffinate) and the TMB model for a mass transfer coefficient of $k = 0.2$ s^{-1} (99.0% pure extract and raffinate). There is no 99.0% separation region using the SMB model with a 1211 configuration and for $k = 0.2$ s^{-1}.

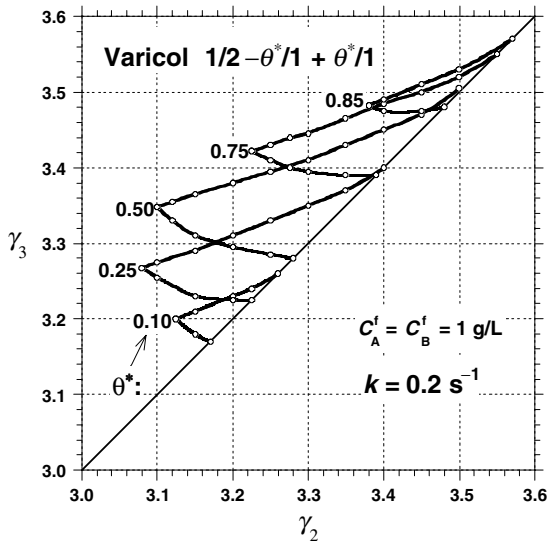

Figure 7.15 $\gamma_3 \times \gamma_2$ separation regions for case 1, feed concentrations of $C_A^f = C_B^f = 1$ g/L, and a mass transfer coefficient of $k = 0.2$ s^{-1} (99.0% pure extract and raffinate). Separation regions obtained using the Varicol operation with a total of five columns and a configuration of $1/2 - \theta^*/1 + \theta^*/1$ configuration, with $\theta^* = 0.10, 0.25, 0.50, 0.75$ and 0.85.

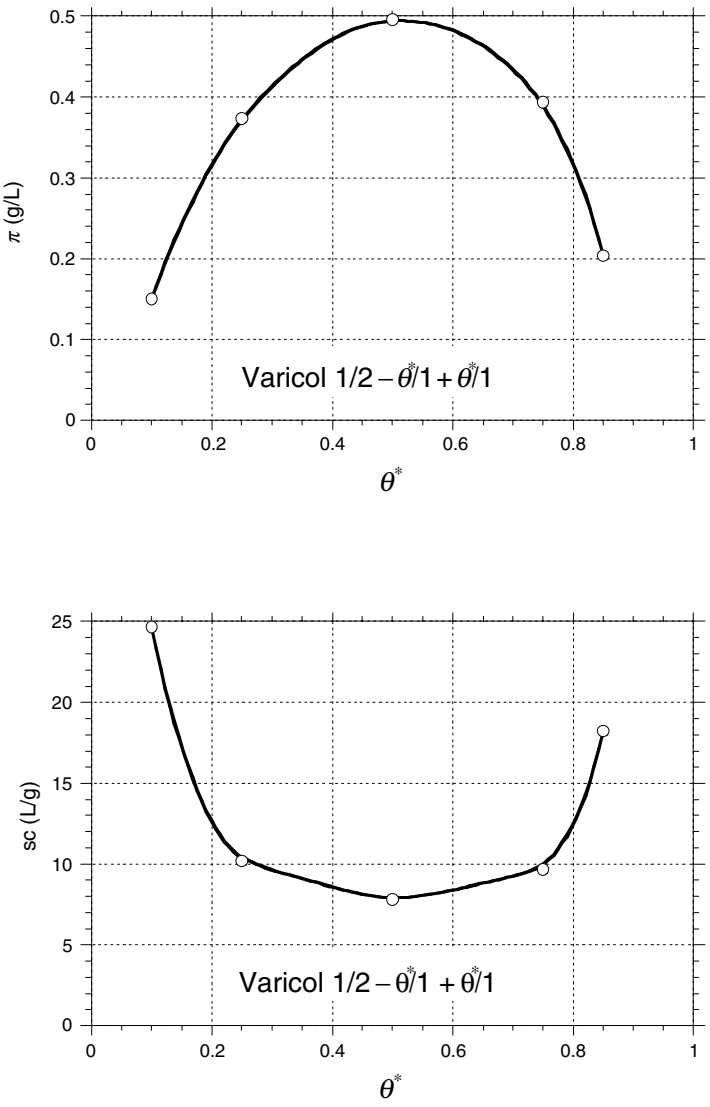

Figure 7.16 Influence of θ^* on the system productivity and solvent consumption for case 1, feed concentrations of $C_A^f = C_B^f = 1$ g/L, and a mass transfer coefficient of $k = 0.2$ s^{-1} (99.0% pure extract and raffinate). System productivity and solvent consumption are evaluated at the vertex points of the separation regions obtained by simulation using the Varicol $1/2 - \theta^*/1 + \theta^*/1$ operation.

In conclusion, the use of SMB units with a low number of chromatographic columns presents the advantage of a simpler and more economic solution, but may lead to a significant loss of process purity or system productivity. The Varicol process, a modification of the classic SMB operation by introducing a nonsynchronous shift of the inlet and outlet lines, can overcome this disadvantages and present performances closer to the ones obtained with SMB units with a higher subdivision of the adsorbent bed.

7.6.2 *Pseudo-SMB processes*

Recently, SMB operation has been modified to allow the separation of ternary mixtures. The process described in this section was proposed by the Japan Organo Company (http://www.organo.co.jp/technology/hisepa/en_hisepa/) using patented technology [28, 29]. This technique of pseudo-SMB chromatography is being applied in the separation of complex multicomponent mixtures, for instance, the separation of beet molasses mixtures into raffinose, sucrose, glucose and betaine [29] and in the production of raffinose from beet molasses [30].

Like SMB, it is also a cyclic process, in which the following two steps constitute one cycle:

(1) In the first step, the feed and eluent streams enter the system and the component B, with intermediate affinity, is recovered. This step can be modeled as a series of preparative chromatographic columns.
(2) In the second step, there is only one inlet flow of eluent and no feed. The more retained component C is recovered in the extract and the less adsorbed species A is recovered in the raffinate. This step can be modeled as a pseudo-TMB with no feed. At the end of this step, the intermediate species B is located downstream of the feed point.

Figure 7.17 shows the traditional TMB system and the schematic diagram of both step 1 and step 2 of the JO process. As described in Section 7.1, in the traditional TMB operation, there are four sections separated by the inlet and outlet streams: section 1, between the eluent and extract ports; section 2, between extract and feed ports; section 3, between feed and raffinate ports; and section 4, between raffinate and eluent ports; the fluid leaving section

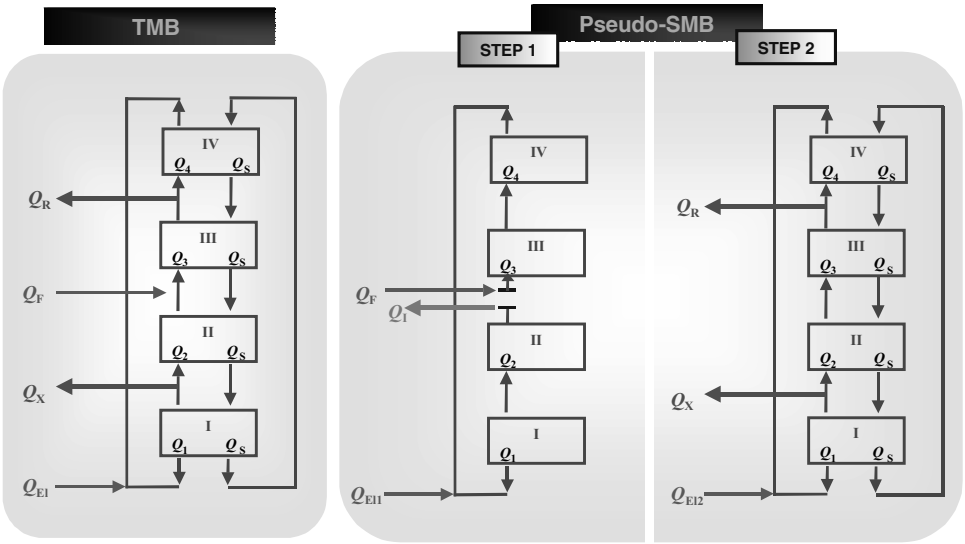

Figure 7.17 Schematic diagrams for TMB and Pseudo-SMB operation.

4 is recycled to section 1. In the pseudo-SMB model of the JO process, we still consider four sections for convenience: in step 1, the feed flows through sections 3 and 4, and the sum of feed plus eluent flow rates flow through sections 1 and 2; in step 2, equivalent to a TMB operation, the flow rates in sections 2 and 3 are the same, since there is no feed. The detailed mathematical model for the JO process can be found elsewhere [31] and use the same assumptions for the TMB and SMB models presented earlier in this chapter (includes axial dispersion and the mass transfer resistance is described by a linear driving force model).

The operating conditions for the pseudo-SMB JO system, i.e. the choice of the internal flow rates in each section and the duration of steps 1 and 2 in order to obtain the desired separation, can be evaluated taking into account the velocity of propagation of concentration of a species i and the constraints for steps 1 and 2.

Conditions for step 1: the duration of the step 1, t_{s1}, is assumed to be the time necessary to feed the intermediate component, B, only in the first column of section 3 on the upstream of the feed. The time t_{s1} can be calculated from the pulse response of a fixed bed.

Conditions for step 2: the determination of the internal flow rates for step 2 are based on the following assumptions: component A (less retained species) moves with the liquid in order to stay centered in the raffinate; component B (intermediate species) moves with the solid in order to stay totally downstream of the feed point in section 2; and component C (more retained species) moves with the solid in order to stay centered in the extract. A more detailed description of the determination of these conditions can be seen in literature [32].

One example of multicomponent separation using the pseudo-SMB JO process was tested using the ternary system shown in Table 7.3. This system represents the separation of three pure components present in sugar molasses, namely sucrose, fructose and betaine. The characteristics of the physical system (from Japan Organo Catalog, 1998) are shown in Table 7.4. The assumed feed flow rate and the duration of step 2 are $Q_F = 350$ mL/min and $t_{s2} = 66$ min [29]. The duration of step 1 is $t_{s1} = 17.8$ min.

Table 7.3 Values of mean retention time, adsorption parameters (linear isotherms) and mass transfer coefficients for the ternary mixture

Component i	$\bar{t}_i$ (min)	K_i	k (s^{-1})
Sucrose (A)	10.76	0.19	0.20
Fructose (B)	13.91	0.44	0.13
Betaine (C)	16.51	0.65	0.11

Table 7.4 Characteristics of the SMB columns for pseudo-SMB operation

Column number (total)	12
Column length (cm)	120
Column diameter (cm)	10.84
Column volume (L)	11.1
Number of columns per section	3
Bed porosity, ε	0.4

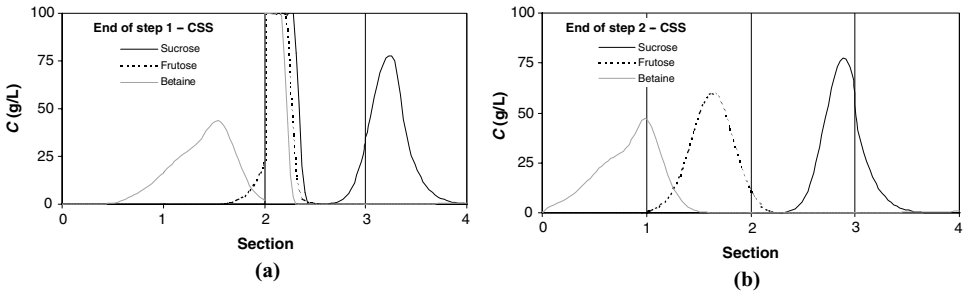

Figure 7.18 Pseudo-SMB operation. Concentration profiles of sucrose, fructose and betaine, at the end of (a) step 1 and (b) step 2. CSS = cyclic steady state.

Figure 7.18 shows the concentration profiles in the liquid phase at the end of (a) step 1 and (b) step 2, obtained after cyclic steady state was achieved. The feed containing the three solutes at species concentration $C_0 = 100$ g/L is injected in step 1 of the cycle during $0 < t \leq t_{s1}$ with flow rate Q_F, at the inlet of section 3. At the same time, there is an intermediate stream, Q_I, rich in fructose, coming out from the end of section 2. During the second step of the cycle for $t_{s1} < t \leq t_{s2}$, the feed flow and the flow of intermediate species are stopped. There are two outlet streams: one at the end of section 1, the extract, Q_X; and the other at the end of section 3, the raffinate, Q_R. At the same time, it is assumed that the solid starts moving in the opposite direction of the fluid. The less retained component, sucrose, moves in the direction of the fluid, but both fructose and betaine move in the opposite direction, i.e. in the direction of the solid phase.

Figure 7.19 shows the movement of each component in the liquid phase during its recovery. Namely, it shows

(a) the evolution of the internal liquid sucrose profile during step 2 (from the end of step 1 to the end of step 2): during this time, t_{s2}, sucrose is recovered at the bottom of section 3, in the intermediate stream;
(b) the evolution of the internal liquid fructose profile during step 1 (from the end of step 2 to the end of step 1): during this time, t_{s1}, fructose is recovered at the bottom of section 2, in the intermediate stream;
(c) the evolution of the internal liquid betaine profile during step 2 (from the end of step 1 to the end of step 2): during this time, t_{s2}, betaine is recovered at the bottom of section 1, in the extract stream.

This example shows how SMB operation can be modified to improve its classical goal of binary to ternary separations.

Notation

b	adsorption isotherm parameter
C	fluid phase concentration
D_L	axial dispersion coefficient
K	adsorption isotherm parameter (linear range)

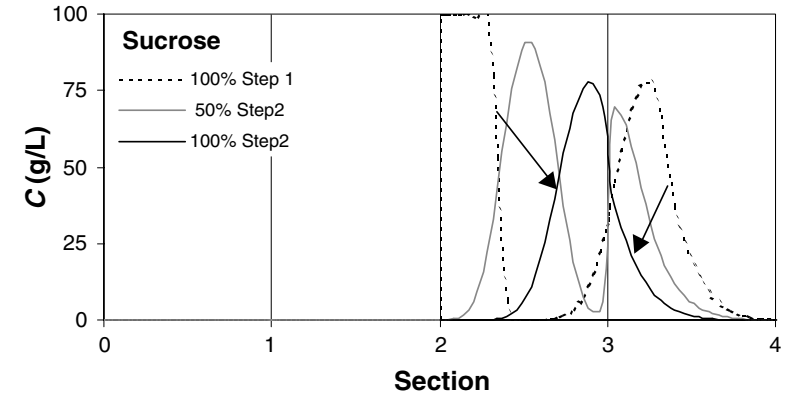

(a)

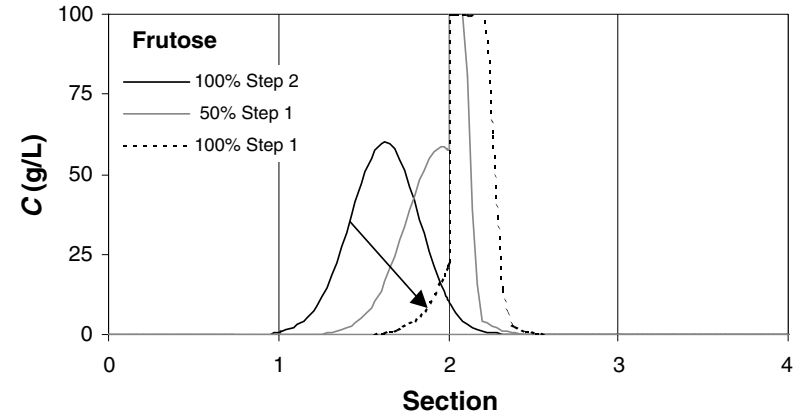

(b)

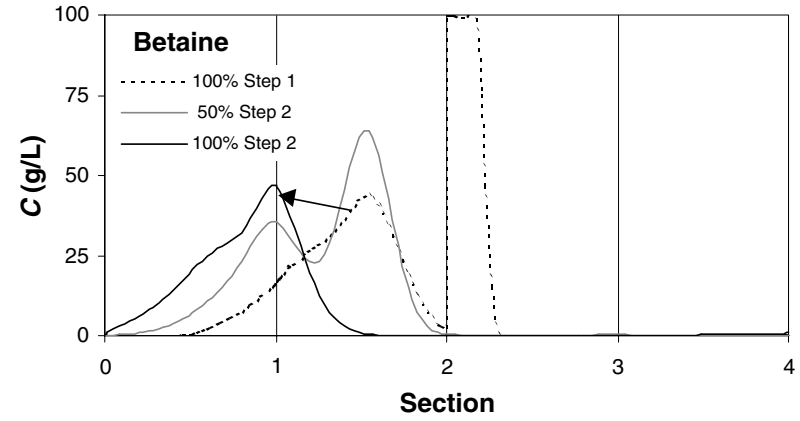

(c)

Figure 7.19 Pseudo-SMB operation. Evolution of the concentration profiles during the recovery of (a) sucrose in step 2, (b) fructose in step 1 and (c) betaine in step 2.

k	mass transfer coefficient
L_c	length of an SMB column
L_j	length of a TMB section
m	adsorption isotherm parameter
n	number of mass transfer units
N_c	total number of columns in the SMB unit
Pe	Peclet number
pr	system productivity, defined as in Equation (7. 17)
Q	adsorption isotherm parameter
Q	volumetric liquid flow rate in the TMB
Q^*	volumetric liquid flow rate in the SMB
Q_s	solid flow rate
q	average adsorbed phase concentration
q^*	adsorbed phase concentration in equilibrium with C
sc	solvent consumption, defined as in Equation (7. 19)
t^*	switch time interval
$\bar{t}$	mean retention time
t_{s1}	duration of the step 1 in the pseudo-SMB JO process
t_{s2}	duration of the step 2 in the pseudo-SMB JO process
u_s	interstitial solid velocity in the TMB operation
V_c	volume of an SMB column
v	interstitial fluid velocity in the TMB operation
v^*	interstitial fluid velocity in the SMB operation
x	dimensionless axial coordinate

Greek symbols

α	selectivity
γ	ratio between fluid and solid interstitial velocities in the TMB operation
γ^*	ratio between fluid and solid interstitial velocities in SMB operation
ε	bed porosity
θ	dimensionless time
π	productivity parameter, defined as in Equation (7. 18)

Subscripts

E	eluent
F	feed
I	intermediate (in pseudo-SMB JO process)
R	raffinate
X	extract
i	component index (i = A, B for binary, or i = A, B, C for ternary systems)
j	section index ($j = 1, 2, 3, 4$)
k	column index ($k = 1, \ldots, N_c$)

References

1. Rodrigues, A.E. and Tondeur, D. (eds), *Percolation Processes: Theory and Applications*, NATO ASI Series, Vol. 33, Sijthoff & Noordhoff, The Netherlands, 1981.
2. Ruthven, D.M., *Principles of Adsorption and Adsorption Processes*, John Wiley & Sons, New York, 1984.
3. Rodrigues, A.E., LeVan, M.D. and Tondeur, D. (eds), *Adsorption: Science and Technology,* NATO ASI Series, Vol. 158, Kluwer Academic Publishers, The Netherlands, 1989.
4. Suzuki, M., *Adsorption Engineering*, Chemical Engineering Monographs, Vol. 25, Elsevier, Tokyo, 1990.
5. Dondi, F. and Guiochon, G. (eds), *Theoretical Advancement in Chromatography and Related Separation Techniques*, NATO ASI Series, Vol. 383, Kluwer Academic Publishers, The Netherlands, 1992.
6. Ganetsos, G. and Barker, P.E. (eds), *Preparative and Production Scale Chromatography*, Chromatographic Science Series, Vol. 61, Marcel Dekker, New York, 1993.
7. Guiochon, G., Shirazi, S.G. and Katti, A.M., *Fundamentals of Preparative and Nonlinear Chromatography*, Academic Press, Boston, 1994.
8. Broughton, D.B., "Bulk separations via adsorption", *Chem. Engng. Prog*., 1977, **73**, 49–51.
9. Broughton, D.B., "Production-scale adsorptive separations of liquid mixtures by simulated moving-bed technology", *Sep. Sci. Tech*., 1984, **19**, 723–736.
10. Broughton, D.B. and Gerhold, C.G., "Continuous sorption process employing fixed bed of sorbent and moving inlets and outlets", US Patent 2,985,589, 1961.
11. Pais, L.S., Loureiro, J.M. and Rodrigues, A.E., "Modeling strategies for enantiomers separation by SMB chromatography", *AIChE J*., 1998, **44**, 561–569.
12. Pais, L.S. and Rodrigues, A.E., "Design of simulated moving bed and varicol processes for preparative separations with a low number of columns", *J. Chromatogr. A*, 2003, **1006**, 33–44.
13. Storti, G., Mazzotti, M., Morbidelli, M. and Carrà, S., "Robust design of binary countercurrent adsorption separation processes", *AIChE J*., 1993, **39**, 471–492.
14. Mazzotti, M., Storti, G. and Morbidelli, M., "Optimal operation of simulated moving bed units for nonlinear chromatographic separations", *J. Chromatogr. A*, 1997, **769**, 3–24.
15. Ruthven, D.M. and Ching, C.B., "Counter-current and simulated counter-current adsorption separation processes", *Chem. Engng. Sci*., 1989, **44**, 1011–1038.
16. Pais, L.S., Loureiro, J.M. and Rodrigues, A.E., "Modeling, separation and operation of a simulated moving bed for continuous chromatographic separation of 1,1′-bi-2-naphthol enantiomers", *J. Chromatogr. A*, 1997, **769**, 25–35.
17. Pais, L.S., Loureiro, J.M. and Rodrigues, A.E., "Separation of enantiomers of a chiral epoxide by simulated moving bed chromatography", *J. Chromatogr. A*, 1998, **827**, 215–233.
18. Azevedo, D.C.S., Pais, L.S. and Rodrigues, A.E., "Enantiomers separation by simulated moving bed chromatography. Non-instantaneous equilibrium at the solid–fluid interface", *J. Chromatogr. A*, 1999, **865**, 187–200.
19. Migliorini, C., Gentilini, A., Mazzotti, M. and Morbidelli, M., "Design of simulated moving bed units under nonideal conditions", *Ind. Eng. Chem. Res*., 1999, **38**, 2400–2410.
20. Biressi, G., Ludemann-Hombourger, O., Mazzotti, M., Nicoud, R.M. and Morbidelli, M., "Design and optimisation of a simulated moving bed unit: role of deviations from equilibrium theory", *J. Chromatogr. A*, 2000, **876**, 3–15.
21. Pais, L.S., Loureiro, J.M. and Rodrigues, A.E., "Chiral separation by SMB chromatography", *Sep. Purif. Technol*., 2000, **20**, 67–77.
22. Azevedo, D.C.S. and Rodrigues, A.E., "Design of a simulated moving bed in the presence of mass-transfer resistances", *AIChE J*., 1999, **45**, 956–966.
23. Azevedo, D.C.S. and Rodrigues, A.E., "Bilinear driving force approximation in the modeling of a simulated moving bed using bidisperse adsorbents", *Ind. Eng. Chem. Res.*, 1999, **38**, 3519–3529.
24. Rodrigues, A.E. and Pais, L.S., "Design of SMB chiral separations using the concept of separation volume", *Sep. Sci. Technol*., 2004, **39**, 241–266.
25. Pais, L.S., Loureiro, J.M. and Rodrigues, A.E., "Separation of 1,1′-bi-2-naphthol enantiomers by continuous chromatography in simulated moving bed", *Chem. Engng. Sci.*, 1997, **52**, 245–257.
26. Adam, P., Nicoud, R.M., Bailly, M. and Ludemann-Hombourger, O., "Process and device for separation with variable-length", US Patent 6,136,198, 2000.
27. Ludemann-Hombourger, O., Nicoud, R.M. and Bailly, M.; "The Varicol process: a new multicolumn continuous chromatographic process", *Sep. Sci. Technol*., 2000, **35** 1829–1862.
28. Ando, M., Tanimura, M. and Tamura, M., "Method of chromatographic separation", US Patent 4,970,002, 1990.

29. Masuda, T., Sonobe, T., Matsuda, F. and Horie, M., "Process for fractional separation of multi-component fluid mixture", US Patent 5,198,120, 1993.
30. Sayama, K., Kamada, T., Oikawa, S. and Masuda, T., "Production of raffinose: a new byproduct of the beet sugar industry", *Zucherind*, 1992, **117**, 893–898.
31. Mata, V.G. and Rodrigues, A.E., "Separation of ternary mixtures by pseudo-simulated moving bed chromatography", *J. Chromatogr. A*, 2001, **939**, 23–40.
32. Mata, V.G., Pais, L.S., Azevedo, D.C.S. and Rodrigues, A.E., "Fractionation of multicomponent sugar mixtures using a pseudo simulated moving bed". In *Proceedings of CHEMPOR'2001 8th Int. Chem. Eng. Conf.*, Aveiro, Portugal, 2001, pp. 567–574.